RadioGraphics

AAPM/RSNA Physics Tutorial for Residents: Topics in US

B-mode US: Basic Concepts and New Technology[1]

Nicholas J. Hangiandreou, PhD

Ultrasonography (US) has been used in medical imaging for over half a century. Current US scanners are based largely on the same basic principles used in the initial devices for human imaging. Modern equipment uses a pulse-echo approach with a brightness-mode (B-mode) display. Fundamental aspects of the B-mode imaging process include basic ultrasound physics, interactions of ultrasound with tissue, ultrasound pulse formation, scanning the ultrasound beam, and echo detection and signal processing. Recent technical innovations that have been developed to improve the performance of modern US equipment include the following: tissue harmonic imaging, spatial compound imaging, extended field of view imaging, coded pulse excitation, electronic section focusing, three-dimensional and four-dimensional imaging, and the general trend toward equipment miniaturization. US is a relatively inexpensive, portable, safe, and real-time modality, all of which make it one of the most widely used imaging modalities in medicine. Although B-mode US is sometimes referred to as a mature technology, this modality continues to experience a significant evolution in capability with even more exciting developments on the horizon.

©RSNA, 2003

Abbreviation: FOV = field of view

Index terms: Ultrasound (US), harmonic study, **.1298[2] • Ultrasound (US), physics, **.1298 • Ultrasound (US), technology, **.1298 • Ultrasound (US), three-dimensional, **.1298

RadioGraphics 2003; 23:1019–1033 • **Published online** 10.1148/rg.234035034

[1]From the Department of Radiology, East-2, Mayo Clinic, 200 First St SW, Rochester, MN 55905. From the AAPM/RSNA Physics Tutorial at the 2002 RSNA scientific assembly. Received February 19, 2003; revision requested March 28 and received April 17; accepted April 21. The author received a loan of equipment and research funding from Siemens Medical Solutions, Issaquah, Wash. **Address correspondence to** the author (e-mail: *hangiandreou@mayo.edu*).

[2]**. Multiple body systems

©RSNA, 2003

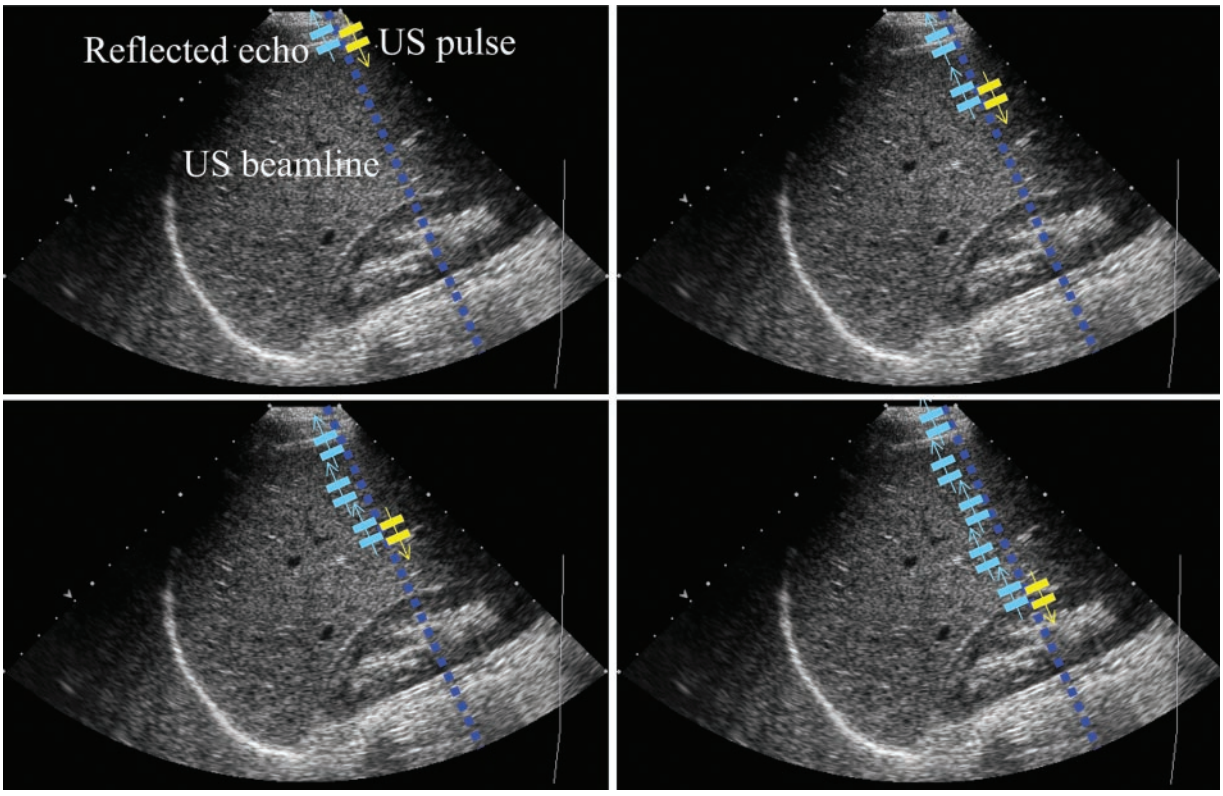

Figure 1. Sequence of diagrams shows the propagation of an ultrasound pulse (yellow arrow) along one particular beam line (dotted line). Echoes (blue arrows) are generated by reflections of the pulse from structures in the tissue medium all along this path, and the echoes travel back to the transducer (not shown).

Introduction

Ultrasonographic (US) instruments have been used to image the human body for at least 50 years. US is currently one of the most important, widely used, and versatile imaging modalities in medicine. US images are tomographic and are acquired at "real-time" rates. The technology is relatively inexpensive and portable, especially when compared with modalities such as magnetic resonance (MR) and computed tomography (CT). Also, as currently applied in the medical environment, US poses no known risks to the patient. These characteristics allow it to be commonly used as a primary diagnostic imaging modality. In addition, the Doppler effect is used to make quantitative measurements of absolute blood velocity and to map blood flow over a large field of view (FOV) in a semiquantitative manner. US is also used extensively to guide many types of interventional procedures. Finally, high-intensity focused US is finding growing use as a therapeutic modality.

Modern medical US is performed primarily by using a pulse-echo approach with a brightness-mode (B-mode) display. This involves transmitting small pulses of ultrasound into the body, detecting echo signals resulting from reflections from structures lying along the path length of the pulse, and then combining the echo signals from many sequential, coplanar pulses into an image. The purpose of this article is to first review the basic principles of B-mode US. This review is not as detailed as other, more extensive treatments of this topic, some of which are noted in the References section (1–4). This review focuses on fundamental aspects of the B-mode imaging process, especially those that are important for understanding the second section of the article, which discusses recent imaging innovations that have been developed to improve the performance of modern US equipment. The review of recent developments includes tissue harmonic imaging, spatial compound imaging, extended FOV imaging, coded pulse excitation, electronic focusing of the image section or plane, three-dimensional and four-dimensional imaging, and the general trend toward equipment miniaturization.

Basic Principles of B-mode US

The basic principles of B-mode imaging are much the same today as they were in the initial instruments developed for medical use. In this section,

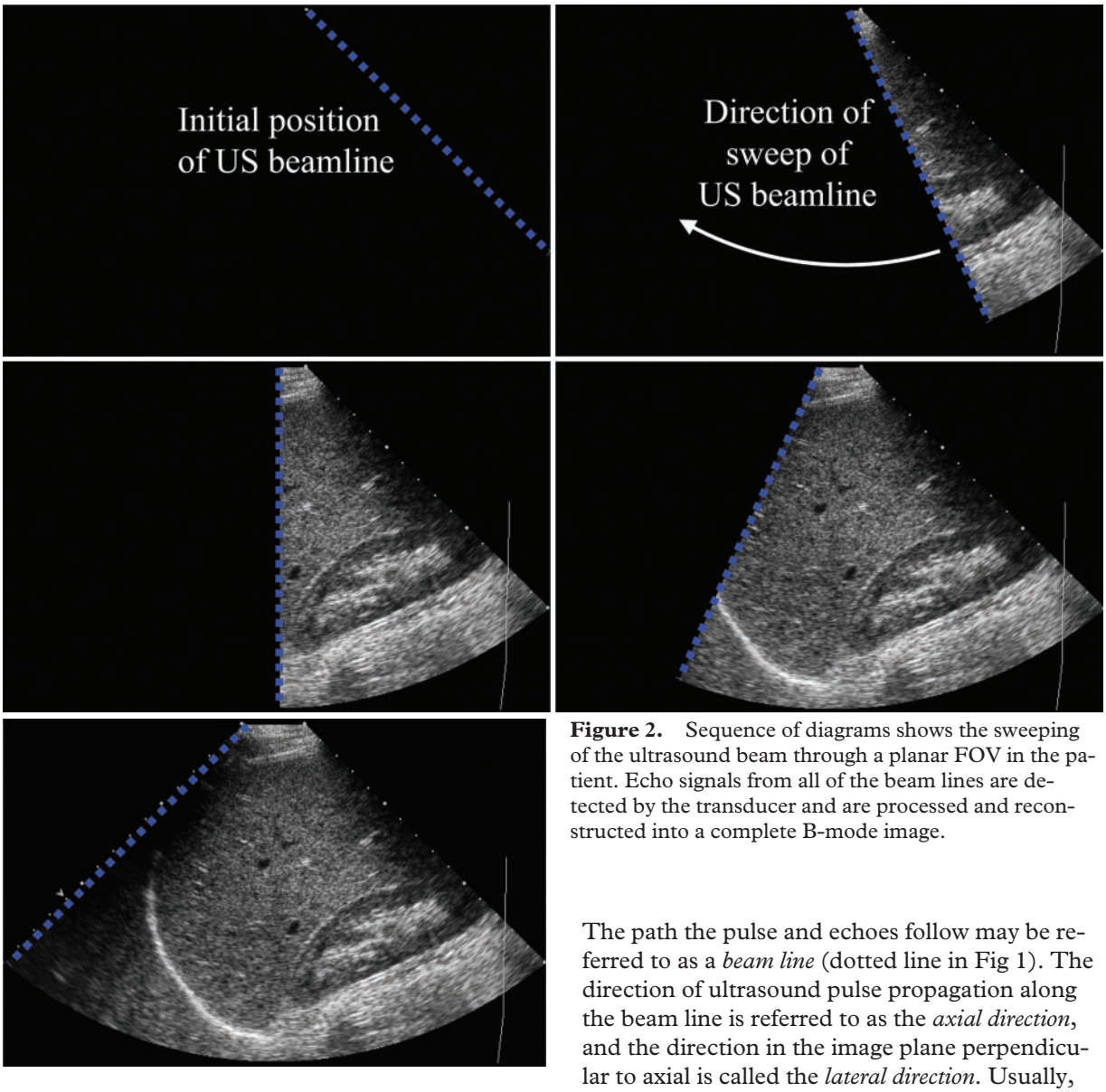

Figure 2. Sequence of diagrams shows the sweeping of the ultrasound beam through a planar FOV in the patient. Echo signals from all of the beam lines are detected by the transducer and are processed and reconstructed into a complete B-mode image.

these basic principles are discussed and the evolution from static to real-time US equipment is reviewed.

General Approach to B-mode US

Medical US is performed by using a pulse-echo approach. This idealized process is illustrated in Figures 1 and 2. A small, spatially localized pulse of ultrasound is produced by a device called a *transducer* (positioned at the top of the US image but not shown in Figs 1 and 2) and is transmitted into the patient. Ultrasound echoes directed back toward the transducer are produced as the pulse travels along a straight line through the tissues. The ultrasound pulse is actually very short (shown in Fig 1 as two thick lines with a perpendicular arrow), but since it traverses a straight path it is often referred to as an *ultrasound beam*. The path the pulse and echoes follow may be referred to as a *beam line* (dotted line in Fig 1). The direction of ultrasound pulse propagation along the beam line is referred to as the *axial direction*, and the direction in the image plane perpendicular to axial is called the *lateral direction*. Usually, only a very small fraction of the ultrasound pulse is reflected as an echo from any point in the patient, with the remainder of the pulse continuing along the beam line to greater tissue depths.

As the pulse travels deeper into the body, in general there will be a long train of echoes en route back toward the transducer, where they will be detected. The different reflectivities of various structures encountered by the pulse cause a corresponding variation of the detected echo strength. The detected echo signals are processed and translated into luminance, resulting in a "brightness-mode" or B-mode image display. In B-mode images, more reflective structures appear brighter than less reflective structures. A complete image is obtained by repeating this pulse-echo cycle for

many coplanar beam lines (Fig 2). Pulses for successive beam lines are transmitted after all of the echoes from the previous beam line have been detected by the transducer. After all of the echoes from all of the beam lines have been detected and processed, these signals are mapped to the proper locations in the image pixel matrix, and the complete B-mode image is displayed. The entire process is immediately repeated to obtain echoes for the next image frame, generally at rates of 20–40 frames per second.

Basic Ultrasound Physics

Ultrasound consists of mechanical waves with frequencies above the upper auditory limit of 20 kHz. Frequency is equal to the number of wave cycles produced each second, and medical US devices commonly use longitudinal waves with a frequency range of about 2–15 MHz. Mechanical waves must travel through some physical medium like air, water, or tissue. These waves correspond to regions in the medium where pressure is alternately higher than and lower than the resting or ambient pressure. Where pressure is high, the medium is squeezed or compressed; where pressure is low, the medium is stretched or rarefied (Fig 3). The medium moves in an oscillatory manner, alternating between states of compression and rarefaction. Each small element of the medium moves back and forth about its resting location but does not undergo any net motion as the wave propagates. The term *longitudinal* refers to waves that cause oscillatory motion of the medium in the same direction as the direction of wave propagation. Transverse waves (shear waves), in which the medium oscillates in a direction perpendicular to the propagation direction, are rapidly attenuated in tissue and so do not play a direct role in medical B-mode imaging.

Another commonly encountered acoustic variable is the acoustic intensity, which is defined as the power per unit cross-sectional area of the ultrasound pulse. Ultrasound that is tightly concentrated or focused has a higher intensity than ultrasound emitted with the same power but spread over a broader area. Intensity is correlated with the likelihood of bioeffects resulting from exposure to ultrasound. Echo pressure amplitudes can vary by a factor of 10^5 or greater (5), so relative pressure and intensity levels are more conveniently discussed in terms of decibels. Relative pressure amplitude expressed in decibels equals $20 \cdot \log(P2/P1)$, where *P1* and *P2* are the two pressure amplitudes being compared. These might correspond to the pressures of an initial ultrasound pulse *(P1)* and an echo from some anatomic structure *(P2)*. Similarly, relative intensity expressed in decibels equals $10 \cdot \log(I2/I1)$. The difference in the leading constants in the two expressions ("20" and "10") is due to the fact that intensity is proportional to the square of the pressure amplitude.

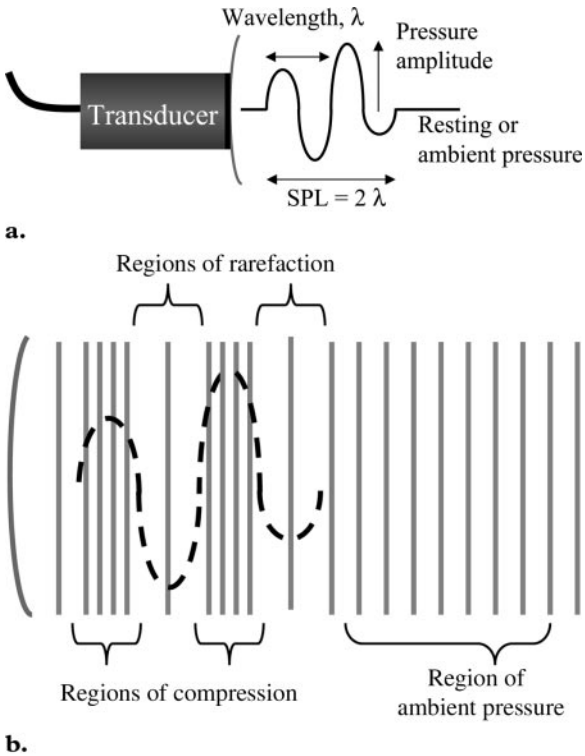

Figure 3. **(a)** Diagram shows an ultrasound pulse that was generated by a transducer and consists of two wave cycles. The spatial pulse length *(SPL)* in this case is equal to twice the ultrasound wavelength. **(b)** Diagram shows tall "elements" of the tissue medium along with the regions that are compressed and rarefied by the pressure oscillations of the ultrasound pulse (dashed line). Regions beyond the extent of the ultrasound pulse are at ambient pressure.

Ultrasound pulses travel through biologic tissues with an average velocity *(c)* of about 1,540 m/sec. The actual velocities in specific tissues vary about this average. For example, the sound speeds of fat, amniotic fluid, kidney, muscle, and skull bone are about 1,450, 1,540, 1,565, 1,600, and 4,080 m/sec, respectively (1). US scanners commonly assume that ultrasound travels through all tissues with a speed of 1,540 m/sec. This assumption is used to compute the depth *(D)* at which detected echoes were produced by rearranging the definition of velocity: D = (time from pulse generation to echo detection) $\cdot$ $c/2$. This expression is commonly referred to as the *range equation*. The factor of "2" results from the fact that the total round-trip path length includes

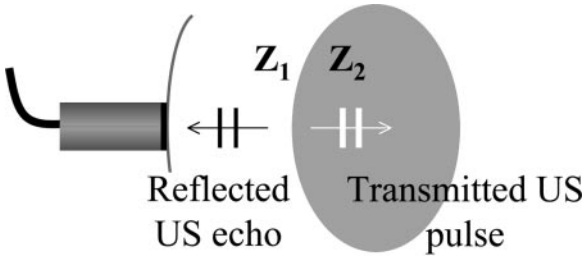

Figure 4. Diagram shows specular reflection with 90° incidence on an interface between two tissues with acoustic impedances of *Z1* and *Z2*.

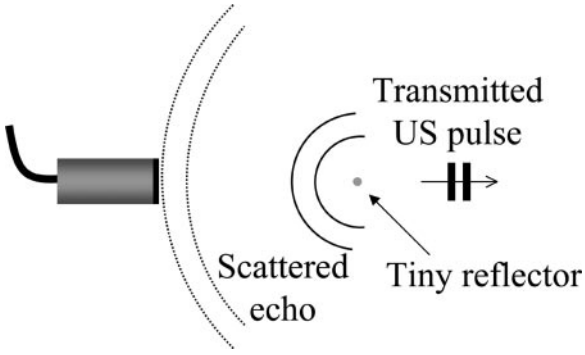

Figure 5. Diagram shows scattering of the ultrasound pulse by a tiny reflective structure. The scattered echo is shown soon after the scattering event (solid lines) and after it has propagated far enough to reach the transducer (dotted lines).

the travel of the pulse from the transducer to the reflector, and then the travel of the echo back from the reflector to the transducer.

Figure 3 illustrates an ultrasound pulse transmitted from a transducer into the body. The ultrasound wavelength (λ) is defined as the length in the medium of a single wave cycle. The wavelength is related to the frequency and speed of sound by the formula $c = f\lambda$. Wavelengths in tissue range from 0.77 mm at 2 MHz to 0.10 mm at 15 MHz.

Interactions of Ultrasound with Tissue

Echo generation results from the interaction of the incident ultrasound pulse with structures in the tissue medium, and there are several specific types of interaction that contribute to this process. Important to all of them is a tissue property called the *acoustic impedance (Z)*. A simplified definition is $Z = \rho c$, where ρ is the density of the tissue. This quantity is more properly called the *specific acoustic impedance* of the medium.

The situation in which an incident ultrasound pulse encounters a large, smooth interface between two types of tissue with different acoustic impedance values is shown in Figure 4. The result is a partially reflected echo that travels back toward the transducer and a partially transmitted pulse that travels deeper into the patient. This type of reflection is called *specular reflection*. The intensities of the reflected and transmitted pulses sum to the intensity of the original incident pulse (ie, energy is conserved in this interaction). For normal (or 90°) incidence, the intensity of the reflected pulse *(Ir)* as a fraction of the incident intensity is given by the expression $Ir = (Z2 - Z1)^2/(Z2 + Z1)^2$. This quantity is called the *intensity reflection coefficient*. The intensity of the reflected echo increases with increasing impedance difference between the two tissues. If the tissues have identical impedance, no echo results. Interfaces between tissues (excluding lung and bone) generally produce very low intensity echoes. For example, among the relatively strong echoes are those generated by a muscle-fat interface ($Ir = 0.015 = 1.5\%$), whereas a pure liver-kidney interface would generate much weaker echoes ($Ir = 0.0004 = 0.04\%$) (1).

If the angle of incidence with the specular boundary is not 90°, the echo will not travel directly back toward the transducer but rather will be reflected at an angle equal to the angle of incidence (just like visible light reflecting in a mirror). The potential exists for the echo to miss the transducer and therefore not be detected. If the interface between the tissues is rough, the echo will be *diffusely reflected* through a wide range of angles. This decreases the detected echo intensity compared with specular reflection but increases the probability that some echo intensity will be detected by the transducer and displayed in the B-mode image. For nonperpendicular incidence on an interface between two media with different speeds of sound, the transmitted wave will not continue along the straight-line path of the incident pulse but rather will be deflected by some angle. This deflection is called *refraction* and is described quantitatively by Snell's law.

If the ultrasound pulse encounters reflectors whose dimensions *(d)* are smaller than the ultrasound wavelength (ie, $d << \lambda$), *scattering* occurs. This results in echoes that are reflected through a very wide range of angles (Fig 5). As in the case of diffuse reflection, the detected echo intensity is greatly reduced because it is spread out over such a wide range. However, this ensures that some echo intensity will be detected by the transducer regardless of the angle of the incident pulse. Most biologic tissues appear in US images as though they are filled with tiny scattering structures. The speckle signal that provides the visible texture in

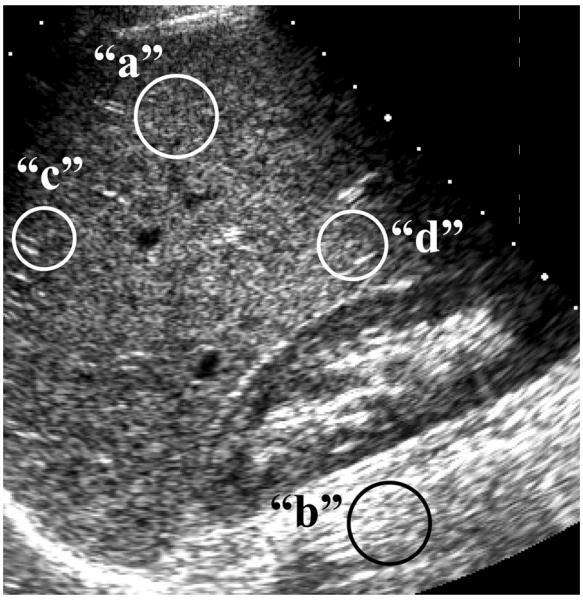

Figure 6. US image shows variation in the appearance of scatter according to the dimensions (regions *a* and *b*) and beam line direction (regions *c* and *d*) of the ultrasound pulse.

organs like the liver (eg, Fig 1) is a result of interference between multiple scattered echoes produced within the volume of the incident ultrasound pulse. Most of the signal visible in US images results from scatter interactions. (In Fig 1, only the portions of the scattered echoes that are directed toward the transducer are schematically shown in light blue.)

The appearance of speckle is closely related to the axial and lateral dimensions of the ultrasound pulse. If the lateral pulse width is greater than the axial pulse length, as is often the case, the speckle "cells" (bright and dark patches of signal) will appear with similar proportions. Varying speckle cell proportions can be observed in regions "a" and "b" of Figure 6. The orientation of the speckle cells will also reflect the orientation of the ultrasound pulses, which is related to their direction of propagation (ie, the direction of the beam lines). This can be observed by comparing regions "c" and "d" of Figure 6. The speckle pattern does not change with time, so successive images obtained through the same plane of the patient with the same transducer position and orientation (ie, beam line directions) will show the same speckle pattern. If the transducer position and orientation are changed, the speckle pattern will generally change as well.

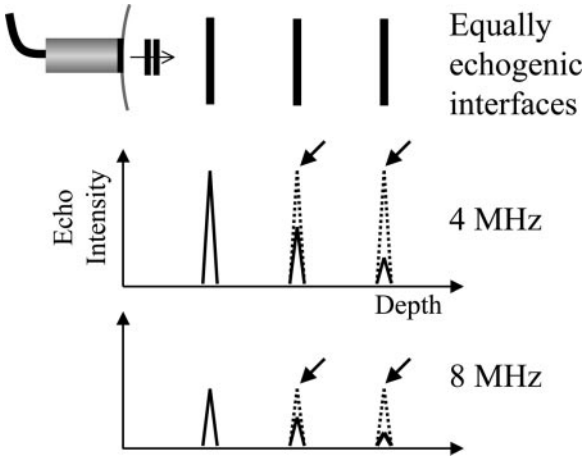

Figure 7. Diagram shows the effects of attenuation on echo intensity from three equally reflective structures. The graphs show echo intensity detected by the transducer (represented by the pulse heights) as a function of reflector depth. Deeper reflectors produce weaker echoes (solid lines) due to increased attenuation over longer path lengths. In addition, attenuation increases (and echo intensity decreases) in proportion to the ultrasound frequency. The dotted lines represent the processed echo signals that result from time-gain compensation (arrows). In this case, all of the signals have the same strength, thus indicating equal reflectivity for the three interfaces, as desired.

As ultrasound pulses (and echoes) travel through tissue, their intensity is reduced or *attenuated*. Attenuation is due to reflection and scattering, which remove intensity from the pulse, from beam divergence and also by friction-like losses. These losses result from the induced oscillatory tissue motion produced by the pulse, which causes conversion of energy from the original mechanical form into heat. This energy loss to localized heating is referred to as *absorption* and is the most important component of ultrasound attenuation. Attenuation through tissue is commonly described as loss of intensity in decibels per centimeter of tissue traversed per megahertz. This is because ultrasound attenuation by tissue is approximately proportional to both the total path length and the ultrasound frequency. Longer path lengths and higher frequencies result in greater attenuation. This is illustrated in Figure 7, which shows the echo intensity detected from three equally reflective interfaces at different depths for two ultrasound frequencies. Attenuation varies between specific types of soft tissue but for the most part occurs in the range of about 0.3–0.8 dB/cm/MHz (5). The frequency dependence of attenuation suggests that to image structures deep in the body, lower US frequencies are required to ensure that adequate echo intensity is detected by the transducer.

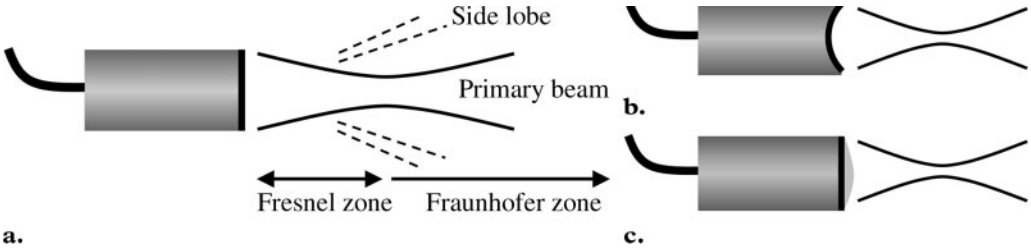

Figure 8. Diagrams show the ultrasound beam profiles from an unfocused transducer **(a)**, a mechanically focused transducer with a curved piezoelectric element **(b)**, and a mechanically focused transducer with an acoustic lens **(c)**. Side lobes are also present for each of the transducers but are shown only for the unfocused transducer **(a)**.

Ultrasound Pulse Formation

The small ultrasound pulses necessary to implement the imaging approaches discussed earlier are produced by devices called *transducers*. In general, a transducer is any device that converts energy from one form into another. One example is a light bulb, which converts electrical energy into light and heat. An ultrasound transducer converts between electrical energy and ultrasound waves (mechanical energy). The most important components of ultrasound transducers are piezoelectric elements, which are fabricated of material with the property that applied electrical signals induce mechanical vibrations and applied mechanical vibrations induce electrical signals. This property is called the *piezoelectric effect*. Composite piezoelectric elements commonly consist of tiny rods of lead zirconate titanate (PZT) ceramic embedded in a matrix of epoxy or similar material. Ultrasound pulses are formed by applying electrical waveforms to the piezoelectric element, causing it to vibrate and emit ultrasound. Echoes are detected when the reflected echo intensity reaches the piezoelectric element and vibrates it slightly. These vibrations are converted by the piezoelectric material into electrical signals.

The pulses discussed so far for US have been short in duration and in extent. The spatial pulse length *(SPL)* in the axial direction is equal to the number of cycles in the pulse multiplied by the ultrasound wavelength (λ). Short pulses are desirable since they generally produce US images with the greatest sharpness in the axial direction (axial resolution). Short pulses are produced by electrically exciting the piezoelectric elements for a very short time, about 1 μsec or less. SPL (and axial resolution) remain constant as the pulse propagates to greater depths.

Similarly, ultrasound pulses that are narrow in the lateral direction produce images with greatest sharpness in that direction (lateral resolution). Narrow ultrasound pulses are produced by focusing the transducer. This may be accomplished for transducers with single piezoelectric elements by curving the element or by using an acoustic lens (made of curved, refractive materials) (Fig 8). These approaches are referred to as *mechanical focusing*. It is also seen in Figure 8 that all ultrasound beams (focused or not) have widths (and lateral resolutions) that vary with distance from the transducer. The point of narrowest width occurs at the focal distance. For unfocused transducers, this point is also called the *near field length*. The region closer than this to the transducer is called the *near field* or *Fresnel zone*, and the more distant region is called the *far field* or *Fraunhofer zone*. These regions are illustrated in Figure 8. Focusing can be accomplished only in the near field of the transducer. For any particular frequency, the mechanical focusing characteristics are fixed as a function of the element curvature or the shape and composition of the lens. Ultrasound pulses with narrower widths at the focal distance, and thus improved lateral resolution, are achieved by using higher ultrasound frequencies. This produces a trade-off, since the higher frequencies that are desired for better spatial resolution also produce increased attenuation and thus weaker echo signals at greater depths.

Also shown in Figure 8a are side lobes. These are unwanted regions of ultrasound intensity that lie off of the main beam axis. They are typically much weaker than the main ultrasound beam but are present for all transducers and have the possibility for causing image artifacts.

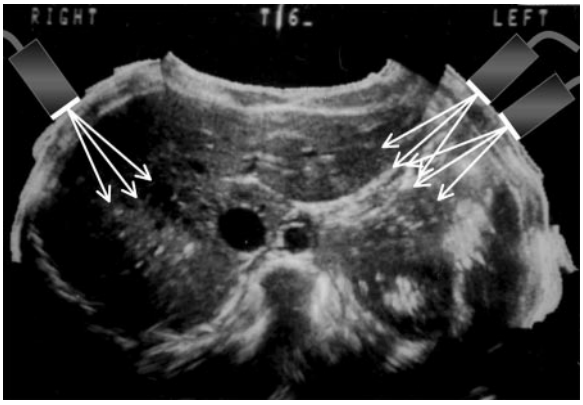

Figure 9. Sample abdominal US image obtained with a manual, static B-mode imager. Also shown are several transducer positions and beam lines that contributed to the image acquisition.

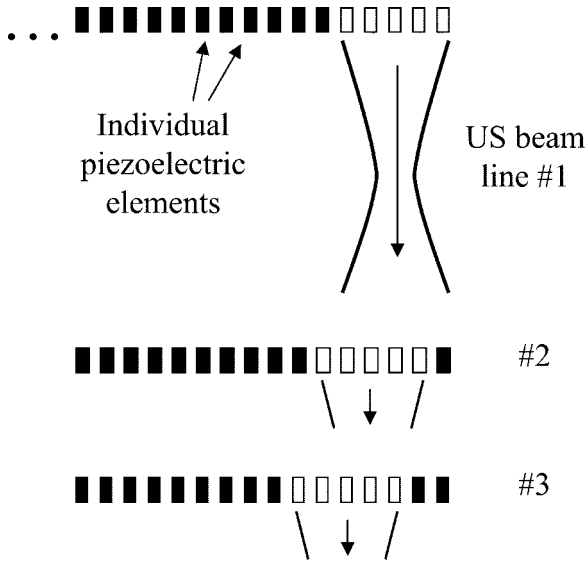

Figure 10. Diagram shows the method of electronic beam scanning for a linear-array transducer.

Scanning the Ultrasound Beam

Early US systems relied on the operator to manually change the position and orientation of the transducer and scan the ultrasound beam through a plane in the patient to obtain the echo data necessary for each image. The transducer was attached to a mechanical position sensor, which constrained the transducer to move in a plane and tracked the transducer position and orientation in space as echoes were being received. This allowed echoes obtained from many individual beam line directions to be registered and combined into a single image. This was a time-consuming process but produced images that covered large FOVs. Image artifacts occurred if the patient moved during the acquisition. A sample image is shown in Figure 9. This figure also shows some of the many transducer locations and beam lines used in obtaining echo data for the image. Multiple beam lines could be obtained from each location by rocking the transducer in the image plane.

Mechanical sector scanners provided automatic image acquisition capability and used a motor in the transducer housing to automatically rotate the beam line through an arc. Full US images were obtained in times of 1/10 second or less. Most modern US imagers automatically scan the ultrasound beam using transducers consisting of arrays of many narrow piezoelectric elements. The array may consist of as many as 128–196 elements (6). In linear-array transducers, the ultrasound beam is created by electrically exciting only a subset of these elements (Fig 10). The ultrasound pulse is emitted perpendicular to the element array and is centered over the element subset. Successive beams are obtained by shifting the subset of excited elements across the face of the array, effectively shifting the beam line laterally by a small amount. Often, a larger subset of elements is used to receive the returning echoes. In this manner, the ultrasound beam can be electronically swept across an entire rectangular field in 1/10 second or faster.

In curvilinear-array transducers, the array of elements is arranged across a convex arc (instead of a straight line), which rapidly scans a sector-shaped FOV. Other types of array transducers (phased arrays and vector arrays) typically are shorter and have fewer elements but excite a much larger fraction of the elements for each beam. The timing is adjusted so that the elements are not all excited simultaneously. Slight offsets in excitation timing are used to electronically steer the beam off at nonperpendicular angles, sweeping out sector-shaped FOVs. Figure 11 illustrates three types of array transducers and sample image FOVs produced by each. It is evident that array transducer FOVs are substantially smaller than those produced by static B-mode scanners (Fig 9). The advantage of more rapid, real-time scanning, and the associated immunity to motion artifacts, outweighs this disadvantage in most cases.

Timing offsets when exciting the array elements, similar to those used to steer the ultrasound beam for vector and phased arrays, are also used in all array transducers to focus the beam in the lateral direction at one or more user-selectable focal distances. Timing offsets are used both when the pulses are generated and when echoes are received to optimize the overall lateral resolution. The transducer aperture (determined by the number of excited array elements) can also be

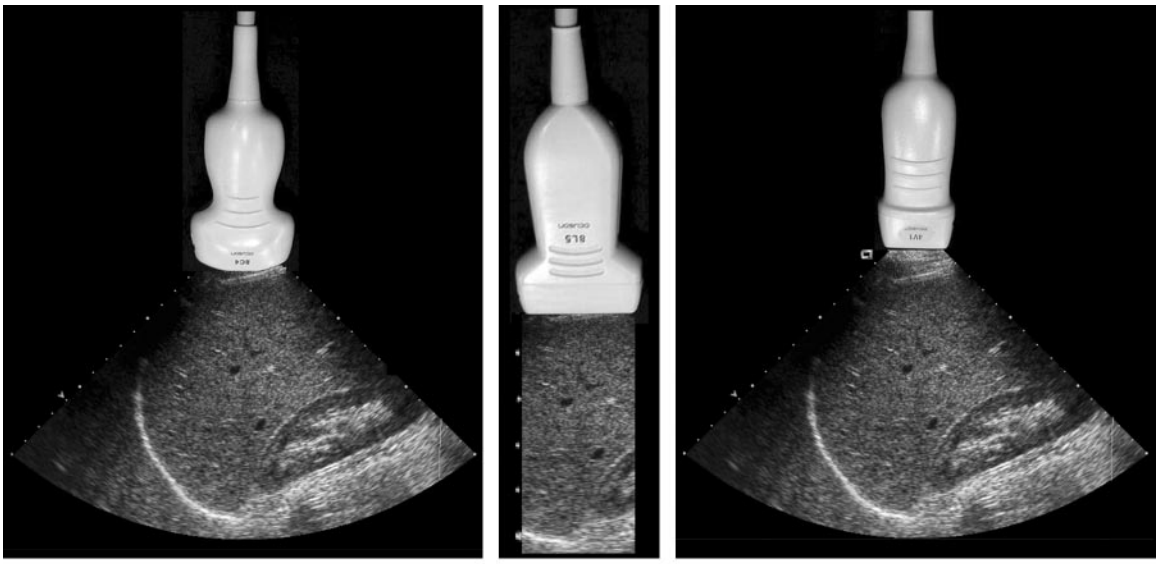

a. b. c.

Figure 11. Photographs show ultrasound transducers with curvilinear **(a)**, linear **(b)**, and vector **(c)** arrays along with sample image FOVs.

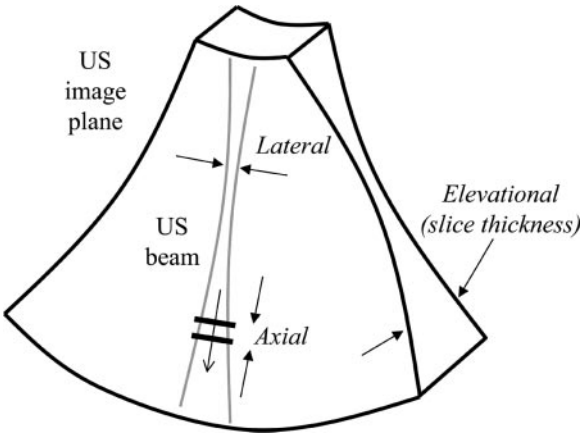

Figure 12. Diagram shows the geometry of the US image plane and the three spatial resolution directions.

dynamically adjusted while receiving echoes to further optimize lateral resolution. Ultrasound beam thickness in the elevational (or section thickness) direction is still commonly controlled by using static mechanical focusing methods. Figure 12 illustrates the geometry of the ultrasound beam and image "plane" for a curvilinear transducer. The thickness of the US image plane is seen to vary with distance from the transducer (ie, the elevational resolution varies with depth, as does the lateral resolution). This figure also shows the three spatial resolution directions: axial, lateral, and elevational.

Echo Detection and Signal Processing

Received echoes are processed by the US scanner in a number of steps. Amplification occurs at several stages. The echo signals are all uniformly preamplified immediately after detection by the transducer, and a uniform user-controllable gain is also applied. In addition, to overcome the effects of attenuation, a depth-dependent gain is applied to the echoes, with echoes originating deeper in the patient (which are attenuated to a larger degree) having larger gain factors than those originating closer to the transducer. The effect of this process is to cause equally reflective structures to be displayed in the B-mode image with the same brightness, regardless of their depth. The corrected echo signals are illustrated by the dotted line peaks in Figure 7. This step is referred to by several names, including *swept gain*, *depth-gain compensation* (DGC), and *time-gain compensation* (TGC).

The dynamic range of the echo signals is also compressed, often via logarithmic transformation. *Dynamic range* refers to the ratio of the largest and smallest signal levels at any particular processing stage. The total dynamic range of detected echo signals can exceed 150 dB. The signal range resulting from depth-dependent amplification may still be 50–60 dB or greater. This signal range is too large to be properly presented on an 8-bit/pixel electronic display, so the dynamic range must be further reduced. This final dynamic range compression step (eg, use of logarithmic transformation) reduces the gain for larger signal magnitudes and increases the gain for smaller signal magnitudes while reducing the overall dynamic range. These signals are also demodulated to remove oscillations at the ultrasound frequency (in the megahertz range), and very small signals are rejected (removed) in an effort to reduce image noise and clutter. The US image may also be

subjected to a variety of processing steps designed to optimize the appearance on the display, sharpen edges, improve contrast, and so on.

Recent Innovations in B-mode US

During the past decade or so, many enhancements to the basic imaging approach presented earlier have been implemented by US equipment manufacturers. These innovations are moving rapidly into widespread use, providing significant improvements in image quality and allowing broader application of the modality.

Tissue Harmonic Imaging

Although discussed herein as a "recent innovation," tissue harmonic imaging has already earned a role as an indispensable, commonly used US mode. The benefits of tissue harmonic imaging were first observed in work geared toward imaging of US contrast materials. The term *harmonic* refers to frequencies that are integral multiples of the frequency of the transmitted pulse (which is also called the *fundamental frequency* or *first harmonic*). The second harmonic has a frequency of twice the fundamental. Ultrasound waves propagate through tissue in a nonlinear fashion. The wave velocity is slightly greater for higher-pressure wave phases than for lower-pressure phases (7). This is illustrated in Figure 13, which shows the net result as a distortion of the ultrasound wave from a perfect sinusoid to a "sharper," more peaked sawtooth shape. This distorted wave contains frequency components centered around many higher-order harmonics (eg, the second, third, fourth). The intensity decreases as the order of the harmonic increases. Also, the higher-frequency harmonic components are attenuated to a greater degree. For these reasons, most harmonic imaging is currently performed by using the second harmonic component.

Stronger harmonic signal components are generated as the ultrasound wave travels through greater tissue path lengths (Fig 13). This means that little harmonic signal originates in the patient body wall close to the transducer. Harmonic images therefore demonstrate good rejection of artifacts and clutter arising from multiple pulse reflections in these near-surface tissues. At greater depths, the harmonic signals will begin to decrease substantially relative to the fundamental signal owing to increased attenuation. Harmonic imaging is generally considered to be most useful for "technically difficult" patients with thick and complicated body wall structures. The strongest

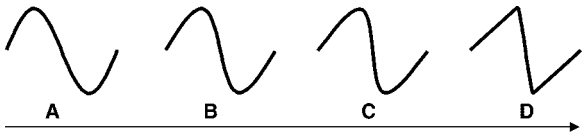

Figure 13. Diagram shows the progressive distortion of ultrasound waves that occurs as the waves propagate through tissue. *A* is the original (undistorted) wave, and *B–D* are the wave shapes that result from propagation through greater tissue path lengths. Wave *D*, which corresponds to the greatest path length, shows the greatest amount of distortion and contains the strongest harmonic signal.

harmonic signals also originate in regions of the ultrasound pulse with the greatest pressure amplitudes, that is, near the pulse center. This often provides harmonic images with superior lateral and elevational resolution relative to fundamental images. An example of the clinical benefits of harmonic imaging is given in Figure 14.

Spatial Compound Imaging

With early static B-mode US scanners, the ability to move and rock the transducer allowed the same regions of the patient to be interrogated with ultrasound beams oriented along different directions (Fig 9). Because the appearance of speckle varies according to the beam line direction, averaging echoes acquired from different directions tended to average out and smooth the speckle, making the images look less grainy. This feature was lost with the transition to mechanical sector scanners and array transducers. Recently, a mode called *spatial compound imaging* has been introduced that restores this speckle reduction capability. Here, electronic steering of ultrasound beams from an array transducer is used to image the same tissue multiple times by using parallel beams oriented along different directions (Fig 15). The echoes from these multiple acquisitions are then averaged together into a single composite image.

Because multiple ultrasound beams are used to interrogate the same tissue regions (instead of just one beam, as in conventional B-mode imaging), more time is required for data acquisition and the compound imaging frame rate is generally reduced compared with that of conventional B-mode imaging. Spatial compound images often show reduced levels of speckle, noise, clutter, and refractive shadows and improved contrast and margin definition (8). Enhancement and shadowing artifacts may also be reduced, which may be an advantage or potential drawback, depending on the imaging situation. Figure 16 shows one example of the clinical advantages of spatial compound imaging.

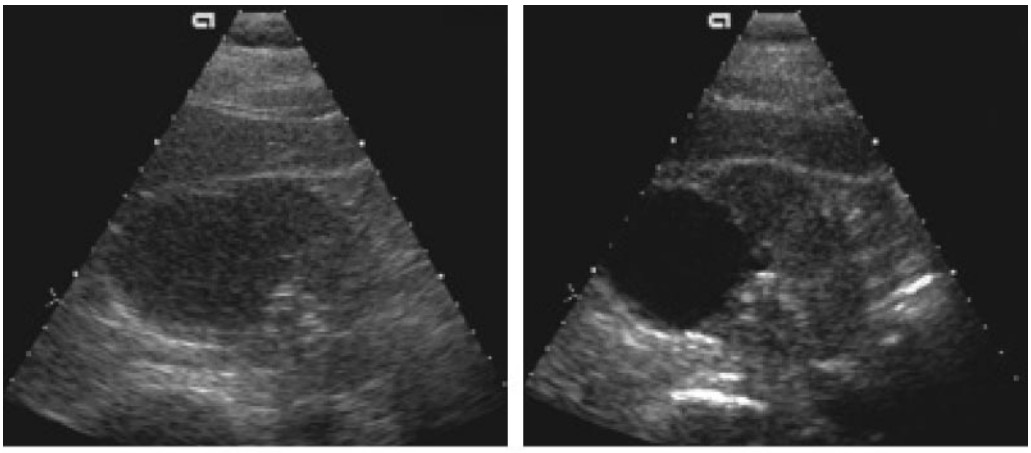

a. b.

Figure 14. Fundamental **(a)** and harmonic **(b)** US images of a renal cyst show the benefits of harmonic imaging. The cyst in the harmonic image **(b)** appears much more anechoic and exhibits sharper, better-delineated margins. (Courtesy of Siemens Medical Solutions, Mountain View, Calif.)

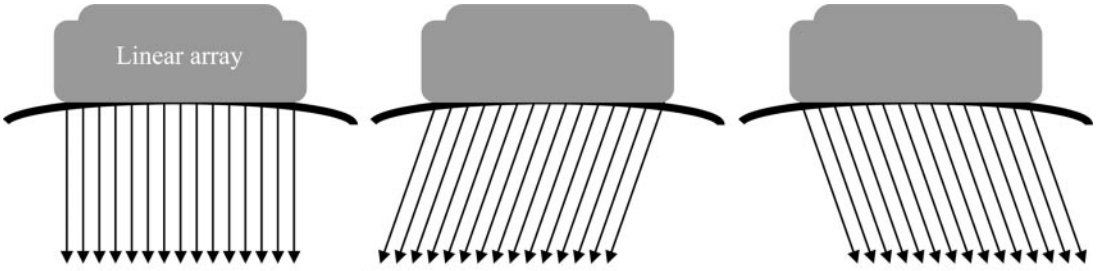

a. b. c.

Figure 15. **(a)** Diagram shows the set of ultrasound beam lines used for conventional B-mode imaging. **(b, c)** Diagrams show two additional sets of beam lines that are used for spatial compound imaging. Data from up to nine such sets of beam lines are acquired and averaged together to form each compound image.

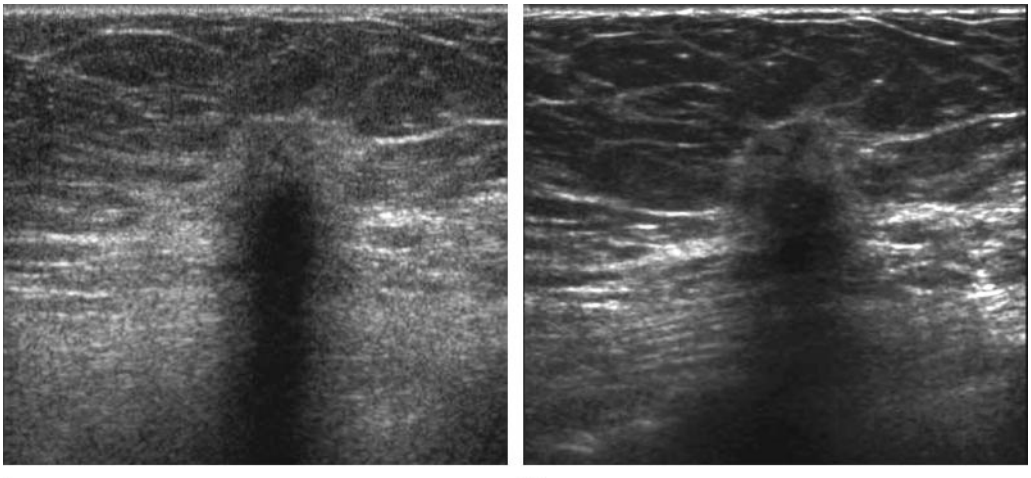

a. b.

Figure 16. Conventional B-mode **(a)** and spatial compound **(b)** US images of a breast mass show the benefits of spatial compound imaging. The mass in the compound image **(b)** is rendered in much greater spatial detail, as are all the tissues in the FOV. In addition, image graininess due to speckle is markedly decreased in the compound image **(b)**. (Courtesy of Philips Ultrasound, Bothell, Wash.)

Extended FOV Imaging

Another benefit of early static B-mode scanners that was lost with the introduction of mechanical and electronic automatic scanning was large imaging FOVs (compare Figs 9 and 11). Another recent US innovation, extended FOV imaging, has sought to restore this capability when imaging with array transducers (9). A sample image is shown in Figure 17. This figure also illustrates the image acquisition process. The transducer is slowly translated laterally across the large anatomic region of interest. During this motion, multiple images are acquired from many transducer positions. The proper relative positions of the multiple images are determined in the scanner by comparison of image data features in the regions of overlap between successive images. This process registers the images with respect to each other, accounting for both translation and (in-plane) rotation of the transducer. The transducer motion during acquisition is reminiscent of static B-mode imaging, but no physical position sensors of any type are required for registration. The registered image data are accumulated in a large image buffer and then combined to form the complete large FOV image. As shown in Figure 17, extended FOV images are not limited just to B-mode acquisitions. Extended FOV imaging restores the capability of visualizing large anatomic regions in a single image and simplifies measurements made over these large regions.

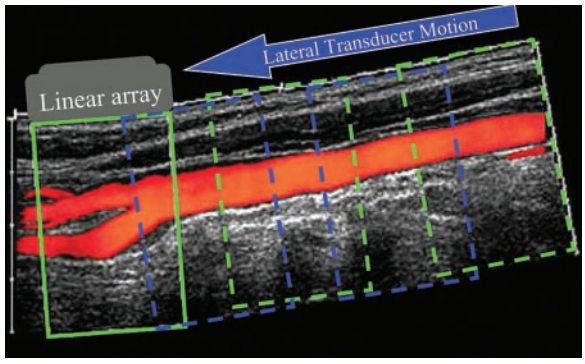

Figure 17. Extended FOV color flow image of the carotid artery shows the data acquisition process. The initial position of the transducer is at the right edge of the large FOV image, and the transducer is moved slowly to the left. The green and blue boxes indicate individual images acquired during this motion, with the solid box representing the last image that contributed to the composite large FOV image. (Courtesy of Siemens Medical Solutions.)

Coded Pulse Excitation

As discussed earlier, a fundamental trade-off in US is that between imaging depth and spatial resolution. Short, highly focused ultrasound pulses that optimize spatial resolution are generally obtained at higher frequencies; however, attenuation of pulse and echo intensity also increases with frequency. It is often the case that suboptimal spatial resolution must be accepted to image with a low enough frequency to produce detected echoes of adequate intensity. Coded ultrasound pulses are a potential means of overcoming this limitation, providing good penetration at the higher frequencies necessary for high spatial resolution (10). In this imaging approach, long ultrasound pulses are used instead of the very short pulses discussed thus far. These long pulses carry greater ultrasonic energy, increasing the energy of echoes that return from large depths in the patient.

Figure 18 shows a comparison between a conventional B-mode pulse and two types of coded pulses. The coded pulses are produced with a very specific, characteristic shape, and the resulting echoes will have a similar shape. Many different pulse shapes are possible. A processing step called *pulse compression* is applied to the detected echo signals, in which the locations of the long, characteristic pulse shapes are identified. These pulse shape locations may be determined with a tight spatial tolerance and are assumed to correspond to the locations of reflective structures in the body. The locations of reflectors may thus be identified with good spatial resolution. The end result is an image with good echo signal and good spatial resolution at large depths. Figure 19 shows an example of the potential clinical advantages of coded pulse excitation imaging.

Electronic Section Focusing

As discussed earlier, electronic focusing of the ultrasound pulse in the lateral direction by using transducer arrays provides great benefits compared with mechanical focusing by using curved piezoelectric elements or acoustic lenses. However, most transducers in current clinical use still employ mechanical focusing in the section thickness direction. The resulting highly variable section thickness (see Figure 12) can cause great difficulty in accurately visualizing small structures. This is illustrated in Figure 20a, which shows a conventional US image of a phantom containing many small anechoic spheres in an echogenic background. The spheres are best visualized only in a relatively small region near the center of the image. Toward the edges of this region, the sphere margins become distorted and the interiors begin to exhibit speckle. Both of these effects are due to larger section thickness causing averaging of overlying echogenic signals with the anechoic spheres.

There is great interest in extending the ability to electronically focus the ultrasound pulse to the

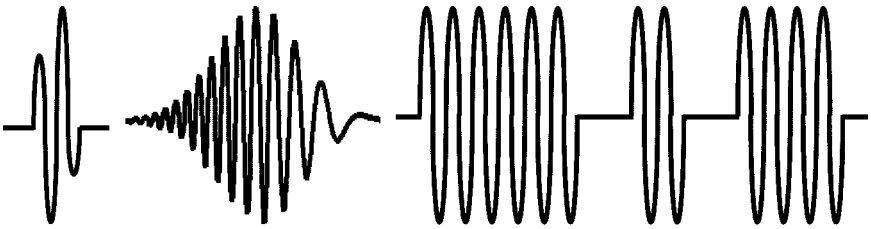

a. b. c.

Figure 18. Diagrams show a typical B-mode pulse **(a)**, a chirp coded pulse **(b)**, and a digitally coded pulse **(c)**.

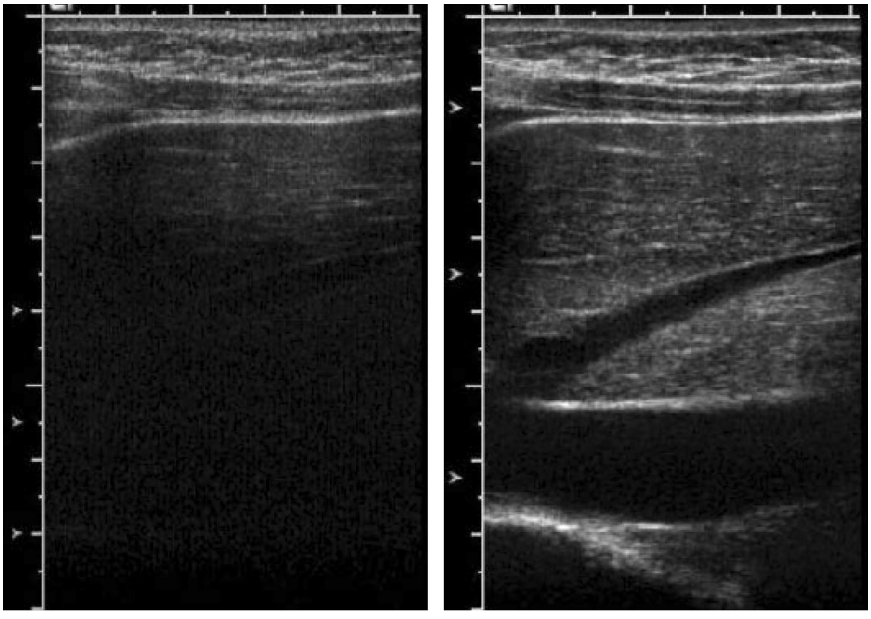

a. b.

Figure 19. Conventional B-mode **(a)** and coded pulse **(b)** US images of the liver show the benefits of coded pulse imaging. The spatial resolution of the coded pulse image **(b)** is very comparable with that of the 13-MHz conventional image **(a)**. However, the useful imaging depth is about 7.5 cm for the coded pulse image **(b)** compared with only about 2.8 cm for the conventional image **(a)**. (Courtesy of Siemens Medical Solutions.)

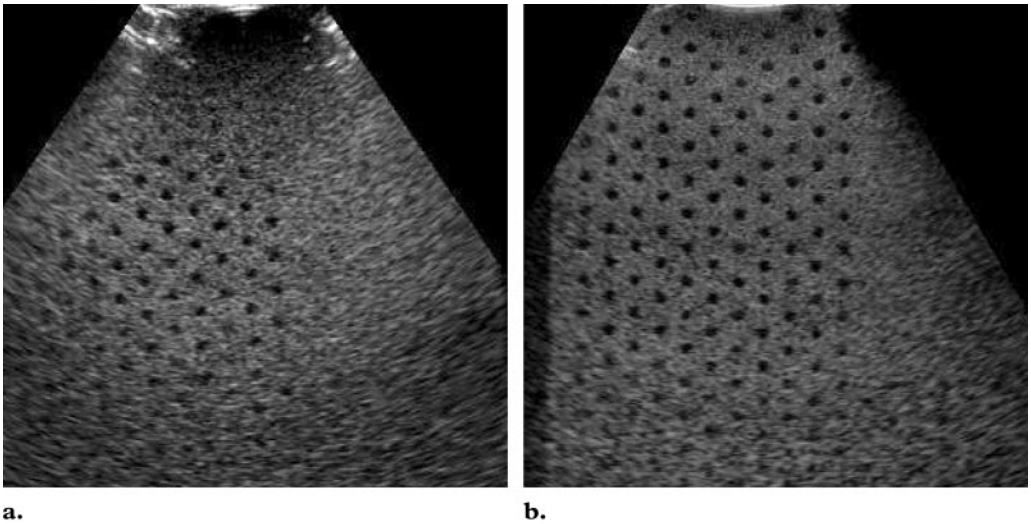

a. b.

Figure 20. US images of a phantom show much improved demonstration of small anechoic spheres in the image obtained with electronic focusing in the section thickness direction **(b)** than in the conventional B-mode image **(a)**. (Courtesy of GE Medical Systems, Waukesha, Wis.)

a. b.

Figure 21. Photographs show commercially available small US scanners from two vendors. **(a)** The upper scanners are 13.3 in (33.8 cm) tall and weigh 5.7 lb (2.6 kg), whereas the lower scanners weigh about 3 lb (1.4 kg). **(b)** The dedicated electronics module attached to the transducer cable weighs 10 oz (0.3 kg) and is 7.6 in (19.3 cm) long. (Fig 21a courtesy of SonoSite, Bothell, Wash; Fig 21b courtesy of Terason, Burlington, Mass.)

elevational direction by using transducer arrays with more than just the one-dimensional single row of piezoelectric elements shown in Figure 10. These higher-dimensional arrays may be referred to as *1.25D*, *1.5D*, *1.75D*, or *full 2D* (two-dimensional) arrays, depending on the number of element rows and the level of independence with which the individual rows may be excited (11). The greater the number of rows, the greater the ability for full electronic focusing. Full 2D arrays will be capable of providing multiple, user-selectable elevational focusing and more uniform section profiles, in addition to electronic steering of the ultrasound beam through a three-dimensional (3D) volume. This electronic focusing and steering will be accomplished by varying timing offsets in the excitation pulses for individual transducer elements, just like in-plane steering and focusing are performed in current array transducers. Full-size, filled 2D array transducers are not yet commercially available; however, smaller versions are just appearing commercially, and 1.25D arrays have been available for several years. Figure 20b shows an image obtained with a transducer that provides electronic section focusing. It is evident that the spherical targets are visualized with better clarity over a much larger region of the phantom.

Three-dimensional US

Freehand approaches to 3D US are currently commercially available on high-end US systems. These methods allow the sonographer to slowly, manually scan the US image plane through a 3D volume in the patient. Features in the individual 2D image data sets can be used to register the various image planes with one another (similar to the approach used for extended FOV imaging), allowing 3D rendered displays of tissue structures. Arguably, the greatest promise for 3D US lies in automated, rapid acquisition of regularly sampled 3D data volumes (with time representing the fourth dimension). This would make US image acquisition similar to MR imaging and CT in that respect. *Four-dimensional (4D) imaging* refers

to the rapid acquisition of a succession of 3D volumes. It is expected that in the long term, beam steering for 3D and 4D acquisitions will be accomplished electronically by using transducers with full 2D arrays of piezoelectric elements. Initially, 1.0D–1.75D transducer arrays (with in-plane electronic beam steering) will be mechanically swept through a volume. At least one dedicated system using this design is now commercially available. Currently, 3D US is most commonly used in obstetric imaging. It is expected that additional clinical applications will develop as these technologies become more widely available.

Miniaturization

Modern full-size US scanners are relatively portable and inexpensive, especially compared with imaging units for modalities such as MR imaging and CT. The general trend toward hardware miniaturization and the use of dedicated integrated circuitry is making possible even smaller and less expensive US scanners, with few (if any) compromises in general image quality and available features. Figure 21 illustrates commercially available small US systems from two vendors. All of the systems shown weigh less than 6 lb (2.7 kg). This trend toward lower cost and smaller systems has great potential to radically alter the overall role of US in medicine.

Conclusions

Modern US equipment is based on many of the same fundamental principles employed in the initial devices used for human imaging over 50 years ago. US has the characteristics of being relatively inexpensive, portable, safe, and real-time in nature, all of which make it one of the most widely used imaging modalities in medicine. Although sometimes referred to as a mature technology, B-mode US continues to experience very significant evolution in capability. In addition, velocity measurement and display capabilities of US instruments are also increasing rapidly, as is the development of new scanning modes, such as US strain imaging. These topics were not treated herein but will be discussed in future articles. In short, US science, technology, and applications are expanding at a brisk pace and are far from mature. Even more exciting developments are on the horizon.

References

1. Zagzebski JA. Essentials of ultrasound physics. St Louis, Mo: Mosby, 1996.
2. Kremkau FW. Diagnostic ultrasound. Philadelphia, Pa: Saunders, 1998.
3. Goldstein A, Powis RL. Medical ultrasonic diagnostics. Physical Acoustics 1999; 23:43–191.
4. Bushberg JT, Seibert JA, Leidholdt EM, Boone JM. The essential physics of medical imaging. Philadelphia, Pa: Lippincott Williams & Wilkins, 2002; 469–553.
5. Carson PL. Ultrasound tissue interactions. In: Goldman LW, Fowlkes JB, eds. Categorical course in diagnostic radiology physics: CT and US cross-sectional imaging. Oak Brook, Ill: Radiological Society of North America, 2000; 9–20.
6. Thomenius KE. Instrumentation for B-mode imaging. In: Goldman LW, Fowlkes JB, eds. Categorical course in diagnostic radiology physics: CT and US cross-sectional imaging. Oak Brook, Ill: Radiological Society of North America, 2000; 21–32.
7. Fowlkes JB, Averkiou M. Contrast and tissue harmonic imaging. In: Goldman LW, Fowlkes JB, eds. Categorical course in diagnostic radiology physics: CT and US cross-sectional imaging. Oak Brook, Ill: Radiological Society of North America, 2000; 77–95.
8. Jespersen SK, Wilhjelm JE, Sillesen H. Multi-angle compound imaging. Ultrason Imaging 1998; 20:81–102.
9. Weng L, Tirumalai AP, Lowery CM, et al. US extended-field-of-view imaging technology. Radiology 1997; 203:877–880.
10. Pedersen MH, Misaridis TX, Jensen JA. Clinical evaluation of coded excitation in medical ultrasound. Ultrasound Med Biol (in press). [A preprint is available at: *http://www.loa.espci.fr/~tmi/en/papers.html*. Accessed April 16, 2003.]
11. Wildes DG, Chiao RY, Daft CMW, Rigby KW, Smith LS, Thomenius KE. Elevation performance of 1.25D and 1.5D transducer arrays. IEEE Trans Ultrason Ferroelectr Freq Control 1997; 44:1027–1037.